JBC Papers in Press. Published on October 7, 2016 as Manuscript M116.733634
The latest version is at http://www.jbc.org/cgi/doi/10.1074/jbc.M116.733634

The C-terminal domains of apoptotic BH3-only proteins mediate their insertion into distinct biological membranes

Vicente Andreu-Fernández [1,2], María J. García-Murria [1], Manuel Bañó-Polo [1], Juliette Martin [3], Luca Monticelli [3], Mar Orzáez [2], and Ismael Mingarro [1]*

From the [1]Departament de Bioquímica i Biologia Molecular, ERI BioTecMed, Universitat de València. E-46100 Burjassot, Spain, the [2]Laboratory of Peptide and Protein Chemistry, Centro de Investigación Príncipe Felipe, Valencia, Spain, and the [3]Bases Moléculaires et Structurales des Systèmes Infectieux (BMSSI), CNRS UMR 5086, 7 Passage du Vercors, 69007 Lyon, France.

Running title: BH3-only protein insertion into membranes

To whom correspondence should be addressed: Prof. Ismael Mingarro, Department of Biochemistry and Molecular Biology, Faculty of Biology A Building, University of Valencia, Dr. Moliner 50, Burjassot 46100, Spain, Telephone: Int+34-96-354 3796, Fax: Int+34-96-354 4635, E-mail: Ismael.Mingarro@uv.es

Keywords: Apoptosis, Bcl-2 family proteins, BH3-only proteins, membrane insertion, membrane protein.

ABSTRACT

Changes in the equilibrium of pro- and anti-apoptotic members of the B-cell lymphoma-2 (Bcl-2) protein family in the mitochondrial outer membrane (MOM) induce structural changes that commit cells to apoptosis. Bcl-2 homology-3 (BH3)-only proteins participate in this process by either activating pro-apoptotic effectors or inhibiting anti-apoptotic components and by promoting MOM permeabilization. The association of BH3-only proteins with MOMs is necessary for the activation and amplification of death signals; however, the nature of this association remains controversial, as these proteins lack a canonical transmembrane sequence. Here we used an *in vitro* expression system to study the insertion capacity of hydrophobic C-terminal regions of the BH3-only proteins Bik, Bim, Noxa, Bmf, and Puma into microsomal membranes. An *Escherichia coli* complementation assay was used to validate the results in a cellular context, and peptide insertions were modeled using molecular dynamics simulations. We also found that some of the C-terminal domains were sufficient to direct green fluorescent protein-fusion proteins to specific membranes in human cells, but the domains did not activate apoptosis. Thus, the hydrophobic regions in the C-termini of BH3-only members associated in distinct ways with various biological membranes, suggesting that a detailed investigation of the entire process of apoptosis should include studying the membranes as a setting for protein-protein and protein-membrane interactions.

Apoptosis, a prevalent mechanism of programmed cell death, is regulated by the Bcl-2 family of proteins. Notably, the balance between pro- and anti-apoptotic Bcl-2 members in the mitochondrial outer membrane (MOM) can protect or trigger MOM permeabilization (MOMP). The members of the Bcl-2 family can be divided into three groups according to their function and the presence of the Bcl-2 homology domains BH1–BH4. One type of pro-apoptotic Bcl-2 family proteins contains only BH3 domain; these proteins are termed BH3-only proteins. Genetic experiments have shown that these proteins are essential initiators of programed cell death (1). Some BH3-only proteins, like Bim, Puma and Noxa, are termed activators, as they directly induce Bax/Bak-dependent MOMP (2,3). Other BH3-only proteins, like Bik, and Bmf, are termed sensitizers, as they promote apoptosis by binding to anti-apoptotic proteins to induce the release of either activator BH3-only proteins (4) or activated Bax or Bak (5).

Several Bcl-2 family members can form membrane channels using amphipathic α-helices, and it is widely accepted that the carboxyl-terminal (C-terminal) hydrophobic domains of these members are inserted into membranes thus anchoring it to intracellular membranes (6), such as the endoplasmic reticulum (ER) and the MOM, where they promote the release of apoptotic factors (7). Since the interaction with the membrane plays an active role in the regulation of apoptosis by changing the affinities of the interactions between partner proteins (8), it would be interesting to determine whether the C-terminal region of BH3-only members targets these proteins to the MOM and/or to ER membranes. In particular, some reports have investigated the anchoring capacity of BH3-only proteins to the MOM (9), although the existence of a transmembrane (TM) region is still being debated.

Bcl-2 family proteins have been cloned and expressed for studies that used high-resolution techniques to give us insights into the physiological control of apoptosis and its pathological consequences (10). However, most of these studies used truncated forms of the proteins that did not include their C-terminal hydrophobic domains. These truncated forms are easier to produce in the larger quantities required for structural studies than the full-length proteins with C-terminal regions; the latter, although more biologically relevant, are difficult to produce (11). A complete understanding of the BH3-only proteins requires studies that investigate the functions of their C-terminal hydrophobic domains. Because individual membrane-inserting α-helices can be considered true protein domains, i.e. independently-folded units with specific functions, the challenge of overexpressing and purifying full-length proteins can be circumvented using a reductionist approach. Specifically, individual C-terminal hydrophobic sequences from BH3-only proteins can be used to evaluate experimentally the targeting and membrane insertion processes.

This study examined the membrane-insertion properties of the C-terminal hydrophobic regions of the human Bim, Puma, Noxa, Bik, and Bmf proteins. When these sequences were analyzed computationally, we found that only the C-terminal domain of Bik was defined *a priori* as a TM segment. However an *in vitro* expression system demonstrated insertion of other low hydrophobicity segments as predicted by coarse-grained molecular dynamics (MD) simulations. Notably, these C-terminal domains were sufficient to determine the intracellular membrane location of chimeric proteins but did not activate an apoptotic response. Taken together, the results of our multifaceted approach suggest that BH3-only proteins can associate with different intracellular membranes in diverse ways that specify their function.

RESULTS

Insertion into ER-derived microsomal membranes – To identify the hydrophobic C-terminal regions of the human BH3-only proteins Bim, Puma, Noxa, Bik, and Bmf, their amino acid sequences were parsed to test the performance of the ΔG Prediction Server (http://dgpred.cbr.su.se/). Given the amino acid sequences, this algorithm predicts the corresponding apparent free energy difference, ΔG_{app}, for insertion of each sequence into the ER membrane by means of the Sec61 translocon (12,13). Table 1 shows the predicted ΔG_{app} values for the C-terminal domains of the analyzed BH3-only proteins. The negative ΔG_{app} value for the Bik C-terminal region predicts a TM disposition, whereas the positive values computed for Bim, Puma, Noxa, and Bmf predict that these sequences do not integrate into membranes.

Next, the membrane insertion capacity of these C-terminal regions was investigated using an experimental system based on Lep, the *Escherichia coli* inner membrane protein leader peptidase. This system accurately reports whether the TM helices are integrated into biological membranes. Since Bcl-2 family proteins are predominantly exposed to the cytosol and anchored to intracellular membranes by their C-terminal regions, in our experimental setup we tested the candidate sequences according to their predicted topology (29). The Lep construct that we used consisted of an extended N-terminal sequence of 24 residues that carries an acceptor site for *N*-linked glycosylation (G1), followed by two TM segments (H1 and H2) connected by a cytosolic loop (P1) then a large C-terminal domain (P2) that contains a second glycosylation site (G2)

(Fig. 1A). This model membrane protein inserts into ER-derived microsomal membranes such that both termini are located in the lumen, allowing co-translational modification of the designed acceptor sites G1 and G2 by the luminal oligosaccharide transferase activity (Fig. 1A). The BH3 C-terminal sequences that we analyzed (BH3-Ct) replaced the Lep H2 domain. In our system, the glycosylation site (G2) located in the first part of the P2 domain can only be modified if the C-terminal domain is translocated across the membrane; in contrast, the G1 site, which is embedded in an extended N-terminal sequence, will always be glycosylated. Single glycosylation (i.e. non-integration of the tested sequence) results in a molecular mass increase of ~2.5 kDa relative to the observed molecular mass of Lep when it is expressed in the absence of microsomes; upon double glycosylation (i.e. membrane insertion of the tested sequence), the molecular mass shifts by ~5 kDa. When proteinase K (PK) is added to the microsomal vesicles, it digests the non-glycosylated form of the P2 domain that is exposed to the cytoplasm (Fig. 1A, right); alternatively, it produces a protected, glycosylated BH3-Ct/P2 fragment when the P2 domain is located in the lumen of the microsomal vesicles (Fig. 1A, left).

In the presence of microsomes, the translation of constructs harboring the Bik C-terminal region (constructed as described previously (30,31)) resulted mainly in double glycosylated forms of the protein (Fig. 1B, lane 5). PK treatment of these samples yielded a protected glycosylated Bik-Ct/P2 fragment (lane 6), indicating that the Bik C-terminal region was inserted into the membrane. Similar results were obtained with constructs harboring the Bmf C-terminal region (Fig. 1C, lanes 7–9). In this case, contrary to the ΔG_{app} prediction (Table 1), the C-terminal region of Bmf was inserted efficiently into the membrane (>60% of the molecules were double glycosylated, with quantification performed as described previously (32)). Regarding the Bim C-terminal region, we found that less than one-fourth of the molecules were inserted into biological membranes (Fig. 1B, lanes 7–9), in good agreement with previous reports in which a portion of the GFP/Bim-Ct fusions localized to the ER membranes (9). Similarly, the Puma C-terminal domain was inserted into microsomal membranes more efficiently than predicted, since up to one-third of the molecules were double glycosylated. Finally, in the presence of microsomal vesicles, the Noxa C-terminal region was single glycosylated and sensitive to PK digestion (Fig. 1C, lanes 4–6), indicating non-TM disposition.

Insertion into E. coli *cellular membranes* – The microsomal *in vitro* system closely mimics the conditions of *in vivo* membrane protein assembly. The C-terminal regions of Bik, Bmf, and, to a lesser extent, Puma and Bim were recognized *in vitro* by the translocon as TM segments out of their native contexts (Fig. 1). We next investigated whether these BH3-only C-terminal regions could direct protein integration into biological membranes in a cellular context. Towards this end, we used an insertion/topology assay into the *E. coli* inner membrane that is based on the function of maltose-binding protein (MBP) in the maltose transport pathway. *E. coli* MM39 cells, which lack endogenous MBP, cannot transport maltose into the cytoplasm for metabolism. Consequently, they cannot grow on media in which the only available carbon source is maltose (17). If the chimeric ToxR(BH3-Ct)MBP is correctly inserted into the inner membrane (Fig. 2A), the periplasmic MBP domain will complement the MM39 *malE*-deficient phenotype and support cell growth on maltose (15). To demonstrate the requirement for periplasmic localization of MBP in the complementation assay we used constructs harboring pro-apoptotic Bax or anti-apoptotic Bcl-2 C-terminal (α_9) TM segments (33) as positive controls and a construct lacking a TM segment (ΔTM) as a negative control. These three controls plus constructs harboring BH3-only C-terminal regions were transformed into MM39 cells and cultured on M9-maltose media, which has maltose as the only carbon source. As shown in Figure 2B, cells expressing the C-terminal regions of Bax, Bcl-2, Bik, and Bmf grew on M9-maltose media. These results demonstrate that both the Bik and Bmf C-terminal-containing constructs anchor their MBP domains to the *E. coli* inner membrane in the correct orientation, which is consistent with the insertion data obtained with the microsomal system. In contrast, cells that lacked a TM segment or that contained the Bim, Puma, or Noxa C-terminal regions failed to grow. The expression of all constructs was verified by growing the cells in complete media with the appropriate antibiotic selection and by immunobloting, using antibodies directed against MBP (Fig. 2C). It should be mentioned

that the C-terminal regions of murine Bim, Puma, and Noxa target chimeric proteins to the mitochondrial membranes, and alkaline extraction experiments suggest membrane insertion rather than peripheral association (9). These apparent discrepancies with our data obtained for human BH3-only protein regions in prokaryotic cells suggest that in addition to sequence differences, there may be eukaryotic proteins or lipid factors that actively assist in the insertion of these three hydrophobic regions into the mitochondrial membranes.

Molecular dynamics simulations of peptide insertion – To help us interpret the protein insertion data, we carried out molecular dynamics simulations of the C-terminal regions from the same five BH3-only proteins (Bik, Bmf, Bim, Noxa, and Puma) plus the H2 domain from Lep in the presence of DOPC lipids. To test the intrinsic tendency of these peptides to insert into lipid membranes, we set up self-assembly simulations for each protein sequence in the presence of DOPC lipids using the MARTINI coarse-grained force field (18,19) assuming an α-helical secondary structure. The amino acid sequence of Puma C-terminal hydrophobic region contains proline residues at position 167 and 180 (residue position in human full-length Puma sequence, Table 1), so we restricted the helical secondary structure to the segment between the proline residues. In all cases, the systems consisted of one copy of the helical peptide, 200 DOPC lipids, and 2180 water particles, all placed in random positions and orientations. In MARTINI simulations, spontaneous lipid self-assembly is observed on short time scales (tens of nanoseconds) due to the very strong driving force (the hydrophobic effect), while the tendency of peptides to be incorporated into a membrane or onto a membrane surface (Fig. 3A) depends essentially on the amino acid sequence (19). As shown in Figure 3B, some peptides, namely Lep-H2, Bik, and Bmf, showed a strong tendency to associate with the lipid membrane and assume a TM orientation (>50% of the cases, Table 1). These were inserted in a TM orientation with over 50% probability. The remaining three peptides, from Bim, Noxa, and Puma, also showed a tendency to insert in a TM orientation, although to a lesser extent (about 40% probability). The agreement with experimental data is reasonable for all of the peptide sequences except for Puma and Noxa. However, in the case of Puma, the simulations predicted a very favorable probability of insertion if a completely helical secondary structure is assumed and a much less favorable probability of insertion for a partially helical conformation (see Table 1). Notably, our simulation methodology did not allow predictions of secondary structure, and peptide insertion prediction depends on the secondary structure of the analyzed peptide. For Noxa we assumed a completely helical secondary structure, and the simulations predicted a significant probability of insertion (close to 40% probability), but no insertion was observed experimentally (Figs. 1 and 2). We hypothesize that this discrepancy can be explained by an incorrect (overestimated) prediction of the secondary structure of Noxa. That is, as observed for Puma, if the peptide is not fully helical, then insertion may be reduced due to the higher polarity of the peptide backbone.

Intracellular localization of BH3-only proteins and apoptotic activity in human cells – There is emerging evidence that the interactions of BH3-only proteins with membranes regulate their binding to other Bcl-2 family members, thereby determining their function (34). Intracellular targeting and localization of the human BH3-only C-terminal regions were evaluated using GFP/BH3-only C-terminus (GFP/BH3-Ct) fusion proteins. Mitotracker dye and the Grp78 protein were used to analyze the ability of the BH3-only C-terminal regions to target a reporter GFP moiety to different cellular organelles in HeLa cells (Fig. 4).

A GFP/Bcl-2 C-terminal fusion protein was used as a positive control for mitochondrial targeting (Fig. 4A). However, some authors have postulated that a fraction of Bcl-2 protein molecules also localize to the ER membrane (35), which is what we observed (Fig. 4B). The C-terminus of human Bim was sufficient for mitochondrial localization of GFP (Fig. 4A), although a portion of GFP/Bim-Ct localized to the ER membranes (Fig. 4B). GFP/Puma-Ct showed similar targeting, whereas the C-terminus of human Bik targeted GFP to the ER, as suggested by previous studies (9,36) (Fig. 4). The C-terminus of human Noxa had no clear membrane-targeting activity (Fig. 4), which is consistent with our membrane-insertion data and with results from a recent study demonstrating that this C-terminal tail serves as a degradation signal in a non-membrane related process (37). The Bmf C-terminal domain showed efficient membrane insertion capacity *in vitro*, *in vivo*, and *in silico* (Figs. 1–3); however, GFP/Bmf-Ct

showed a cytosolic pattern rather than localization to the mitochondrial membrane (Fig. 4A) or to the ER (Fig. 4B).

The biochemical function of BH3-only proteins as essential initiators of intrinsic apoptosis has been largely analyzed (34). However, the role played by their C-terminal hydrophobic regions remains controversial. Previous studies have demonstrated that in the absence of the rest of the protein, the C-termini of some Bcl-2 family members can destabilize the MOM (38) and/or generate pores (39) that release apoptogenic components. More recently, we reported that C-terminal TM peptides from different Bcl-2 family proteins enhance the apoptotic pathway induced by chemotherapeutic agents (7). To test the function of these BH3-only C-terminal regions, we examined whether GFP/BH3-Ct fusions induced apoptosis by measuring caspase activation and cytochrome *c* (cyt *c*) release. As shown in Figure 5, overexpression of the GFP/BH3-Ct fusions in HeLa cells did not induce significant caspase-like activity in either case. In addition, we found no evidence of cyt *c* release by confocal microscopy (data not shown). Collectively, these results show that overexpression of the C-termini of these BH3-only proteins did not induce apoptosis in healthy cells, indicating that the activator or sensitizer activities of BH3-only proteins may require intra-molecular interactions between the C-terminus and the soluble domain of the protein and/or the presence of apoptotic stimuli.

DISCUSSION

Structural and biophysical studies have been invaluable in deciphering the role of BH3-only proteins in apoptosis (40), but gaps remain in our knowledge, especially concerning the ways in which BH3-only proteins influence Bax/Bak membrane associations (41). BH3-only proteins are crucial in the regulation of apoptosis, either by inhibiting anti-apoptotic Bcl-2 family members or by directly activating the pro-apoptotic effectors Bax and Bak (42). In this dual action mechanism, the membrane association and intracellular distribution of BH3-only proteins, especially their MOM localization, can be critical. Towards this end, the C-terminal hydrophobic regions can play a key role in the targeting and sorting of BH3-only proteins. These C-terminal regions have moderate to low hydrophobicity scores, except for the Bik protein, but this does not preclude their insertion into lipid membranes (Figs. 1–3). Notably, all of the C-terminal sequences that we analyzed lacked the flanking positively-charged residues that have been extensively described as mitochondrial targeting signals (43).

Our results showed that the C-termini of the sensitizers Bik and Bmf, and to some extent, those of Puma and Bim, were inserted into biological membranes *in vitro*. Similar results were obtained in the bacterial maltose-complementation system and in coarse-grained simulations. The presence of proline residues within the hydrophobic region of Puma may actually introduce kinks into the helical structure, thereby increasing the polarity for the peptide backbone carbonyl groups about three and four residues N-terminal of the proline location within the helices (44). Increasing the backbone polarity reduces the insertion efficiency of TM helices (45,46). This was confirmed by simulations, which showed that a reduced helical length decreased the probability of peptide insertion (Table 1). The dispersion of charged residues, especially in the case of the Bim C-terminal sequence, would explain the predicted penalty for insertion into the core of the bilayer (Table 1). Nevertheless, the hydrophobic contribution of the neighboring residues in this sequence may compensate, at least partially, for the free energy cost of inserting charged residues into the membrane, as observed previously for some model hydrophobic/cationic sequences (30). This would allow the level of insertion that we observed. In the case of the C-terminal sequence of Noxa, its short hydrophobic region could explain why it was not inserted into the membrane, since the biophysics of hydrophobic mismatch control insertion through the Sec61 translocon of short helices into the ER membrane (46,47).

When these BH3-only C-terminal regions were tested in healthy human cells, some differences were observed. In terms of intracellular localization and insertion, the Bik C-terminus was targeted and inserted into the ER membrane (Fig. 4), in good agreement with previous reports (9,36). Similar to murine sequences, the C-termini of human Bim and Puma appeared to target GFP/Bim-Ct and GFP/Puma-Ct fusion proteins to organelle membranes (i.e. to mitochondrial and ER membranes), whereas the rest of the Bim and Puma proteins, i.e. the soluble domains, are

probably required for efficient mitochondrial localization. Interestingly, the GFP/Bim full-length construct co-localizes with the MOM marker protein Tom20, while constructs containing only the C-terminal stretch of Bim localize to membranes, but not specifically to mitochondrial membranes (48), which is in good agreement with current observations (Fig. 4). This intracellular distribution correlates with their apoptotic function as direct activators of Bax and Bak in the MOM (49).

The GFP/Noxa-Ct fusion protein showed a punctate pattern on fluorescence microscopy (Fig. 4). Together with our *in vitro* and *in vivo* data on protein insertion (Figs. 1 and 2) and recent studies suggesting that the C-terminus of Noxa regulates protein stability through an ubiquitin-independent mechanism (37), it is reasonable to propose that the C-terminus of human Noxa has no membrane targeting/insertion activity. Finally, in contrast to what we found in our membrane insertion assays and molecular dynamics simulations, the cytosolic distribution of GFP/Bmf-Ct indicated that the C-terminus of human Bmf did not contain membrane-targeting information in the absence of apoptotic signals. In fact, the sensitizer Bmf has been proposed to be largely unstructured under physiological conditions and to undergo a conformational change when it is bound to anti-apoptotic proteins in solution (50). Coupled folding and binding could help displace the BH3-only C-terminal domain and target the complex to intracellular membranes (51) in which the Bmf C-terminal region is inserted. In fact, some Bmf isoforms containing the C-terminal hydrophobic region have been found preferentially in the MOM in healthy cells (52).

The human Bik, Noxa and Bmf C-terminal domains that we analyzed were localized mainly to the ER membranes and the cytosol, suggesting that some BH3-only proteins require their soluble domains and/or the recruitment of additional factors to reach the MOM (42). Furthermore, physical interactions between the ER and mitochondrial membranes could allow lateral diffusion of apoptotic signals through BH3-only C-terminal domains that are inserted in ER membranes (53).

To summarize, BH3-only proteins exert their pro-apoptotic function in different ways, and their C-terminal regions have different capabilities in terms of targeting and insertion into intracellular membranes. Once in the MOM, interactions between the BH3-only C-terminal hydrophobic regions with the TM segments from pro-apoptotic (Bax or Bak) and/or anti-apoptotic (Bcl-2, Bcl-x_L, etc.) proteins could modulate mitochondrial apoptosis signaling, most likely by directly or indirectly promoting MOM pore formation. Further studies are needed to fully elucidate the mechanisms that control the apoptotic activation mediated by BH3-only proteins. Such studies should focus on the membrane environment in order to expand our knowledge of this puzzling and well-orchestrated process.

EXPERIMENTAL PROCEDURES

Computer-assisted analyses of BH3-only protein sequences – Putative insertion of hydrophobic regions from BH3-only proteins was predicted using the ΔG Prediction Server v1.0 (http://dgpred.cbr.su.se/) using standard parameters combined with subsequent detection of the lowest apparent free energy differences (ΔG_{app} values) (12,13). The complete protein sequences were obtained from UniProt (http://www.uniprot.org).

Enzymes and chemicals – All enzymes, as well as plasmid pGEM1, and the TNT SP6 Quick Coupled System were from Promega (Madison, WI, USA). ER rough microsomes from dog pancreas were from tRNA Probes (College Station, TX, USA). [^{35}S]Met/Cys was from Perkin Elmer, and restriction enzymes were purchased from Roche Molecular Biochemicals unless otherwise stated. The DNA purification kits were from Thermo Fisher Scientific (Ulm, Germany). All oligonucleotides were purchased from Sigma-Aldrich (Switzerland).

DNA manipulations – For the expression of Lep-derived constructs containing human BH3-only protein C-termini from the pGEM1 plasmid, the Lep sequence carried one glycosylation acceptor site at positions 3–5 of an extended sequence of 24 residues that was described previously (14). Oligonucleotides encoding the different BH3-only C-terminal hydrophobic regions were introduced by replacing the Lep H2 TM segment. Pairs of complementary oligonucleotides (25 μM) were first annealed at 85 °C for 10 min in annealing buffer (20 mM Tris-HCl, 20 mM $MgCl_2$, 500 mM NaCl) followed by slow cooling to 30 °C, after which the two annealed double-stranded

oligonucleotides were mixed, incubated at 65 °C for 5 min, cooled slowly to room temperature, purified and treated with polynucleotide kinase at 37ºC for 30min. The annealed oligonucleotides with *Spe*I/*Kpn*I restriction sites flanking the hydrophobic sequence were ligated overnight with T4 DNA ligase (Promega) at 16°C into purified pGEM-Lep plasmid digested with *Spe*I/*Kpn*I and treated with alkaline phosphatase (Promega). All BH3-derived segment inserts were confirmed by sequencing the plasmid DNA.

To generate maltose-complementarity chimeric constructs, DNA oligonucleotides encoding the putative TM regions of BH3-only proteins were designed and cloned into the pGL3 ToxR-HA-MBP plasmid as described above, in this case the TM sequences were flanked by *Hind*III/*Xho*I restriction sites.

The *Bgl*II and *EcoR*I sites were used as cloning sites for the GFP/BH3-Ct fusions. A template containing all the putative TM sequences flanked with *Bgl*II/*EcoR*I was created with the Gene-art gene synthesis service of Thermo-Fisher Scientific. After PCR amplification, the PCR products were purified, digested, and ligated to the corresponding GFP vector (Addgene #17999) that had been digested with *Bgl*II and *EcoR*I using standard molecular biology protocols. All of the ligated constructs were transformed into *E. coli* DH5α electrocompetent cells, incubated in SOC for 45 minutes at 37°C, pelleted at 3,000×g, and plated directly onto LB agar petri dishes containing ampicillin (50 μg/ml). After 24 h, positive colonies were isolated and cultured on LB medium with ampicillin for 24 h at 37°C. Plasmid DNA was isolated using the GeneJet Plasmid miniprep kit (ThermoFisher Scientific) for sequencing analysis. All new constructs were confirmed by DNA sequencing.

In vitro *transcription/translation assays* – The pGEM1-derived constructs were transcribed and translated using the TNT SP6 Quick Coupled System (Promega). The reactions contained 75 ng DNA template, 0.5 μL ^{35}S-Met (5 μC$_i$), and 0.25 μL microsomes (tRNA Probes) and were incubated for 90 min at 30°C. The translation products were ultracentrifuged (100,000×g for 15 min) on a sucrose cushion, and analyzed by SDS–PAGE. The bands were quantified using a Fuji FLA-3000 phosphoimager and Image Reader 8.1j software. The membrane-insertion probability for a given BH3-segment was calculated as the quotient of the intensity of the double glycosylated band divided by the summed intensities of the single glycosylated band plus the double glycosylated band.

For the proteinase K protection assay, 2 μL of proteinase K (1 mg/mL) was added to the sample, and the digestion reaction was incubated for 15 min on ice. Before SDS-PAGE analysis, the reaction was stopped by adding 1 mM phenylmethanesulfonylfluoride.

ToxR/BH3-Ct/MBP complementation assay – The design and expression of chimeric ToxR/maltose binding protein (MBP) harboring BH3-only C-terminal regions in *E. coli* MM39 cells have been described previously (15-17). Constructs were introduced into chemically competent MM39 cells and plated onto M9 agar plates containing 0.4% maltose, 1% ion agar, and ampicillin (50 μg/mL). For Western blots, MM39 transformants were grown for 2h in LBA liquid media. Cells were lysed by three rounds of freeze–thawing in TBS buffer containing 1% NP-40. The lysates were mixed with SDS-PAGE sample buffer, heated to 95°C for 5 min, separated on 12% (w/v) mini-gels, blotted onto nitrocellulose membranes, and the membranes were blocked with skim milk. The ToxR(BH3-Ct)MBP chimera were detected with HRP-conjugated anti-MBP monoclonal antibody (New England Biolabs) and ECL reagent (GE Healthcare). Chemiluminescence was visualized using an ImageQuant LAS 4000 (GE Healthcare).

Molecular dynamics simulations – All-atom structures for the 6 peptides were generated using Modeller (v9.12). The structures were converted to the MARTINI coarse-grained representation (18,19) using standard scripts that are available on the MARTINI website (http://md.chem.rug.nl/). For self-assembly simulations, we used cubic simulation boxes (8.5-nm lateral size) filled with 1 peptide, 200 DOPC lipids, and 2180 water particles distributed randomly. The α-conformation of the peptides was fixed. For Puma, we performed an additional set of simulations in which only residues 5–14 were in a helical conformation. For each peptide, 100 copies of the simulation system were prepared, each one with a different random distribution. Moreover, two sets of simulations were performed that used the same setup but different versions of the force field i.e. the "standard" v2.2 and v2.2P, including the MARTINI polarizable water model (20). The

total number of simulations was 100*2 for each peptide.

All simulations were carried out with the GROMACS (v5.0) software package (21,22). The Verlet cut-off scheme (using buffered neighbor lists) was used for the calculation of non-bonded interactions (23). Non-bonded forces were calculated with a cut-off of 1.1 nm and shifted functions (24). The dielectric constant was set to 15 when using the standard MARTINI water model and to 2.5 when the polarizable force field was used (20). In simulations with the polarizable water model, the PME method was used for the calculation of long-range electrostatics (25,26). The leap-frog algorithm was used for integration of the equation of motion with a time step of 20 fs. The Bussi-Donadio-Parrinello thermostat (27) was used to maintain a constant temperature of 300 K with a time constant of 1 ps. All simulations were carried out in two steps. During the first step, isotropic pressure coupling was applied (Berendsen algorithm (28), pressure of 1 bar, time constant of 5 ps, compressibility of $4*10^{-5}$ bar^{-1}). The membrane self-assembled during this step, and at the end of the step, the system was rotated to align the membrane normal to the Z axis. In the second simulation step, semi-isotropic pressure coupling was used with the same parameters as in the first step to allow peptide reorientation in or on a tension-less membrane. The duration of each simulation steps was 100 ns for the standard MARTINI model (total simulation time: 7*100*2*100 ns = 140 μs) and 500 ns for the polarizable model (total simulation time: 7*100*2*500 ns = 700 μs).

Cell lines and cultures – Human cervix adenocarcinoma (HeLa) cells were obtained from the ATCC. Cells were grown at 37°C in a 5% CO_2 atmosphere in Dulbecco's modified Eagle's medium plus 10% FBS (GIBCO BRL Life Technologies). The GFP protein was fused at the N-terminus of the putative TM regions of the different BH3-only proteins as described above, and constructs were transfected using LipofectamineTM 2000 (Invitrogen) following the manufacturer's protocol.

Immunofluorescence of GFP/BH3-Ct fusions in HeLa cells – For confocal microscopy, 2×10^5 HeLa cells were seeded on glass coverslips to reach 50% confluence the next day. The cells were transfected as indicated below. To analyze the mitochondrial localization of the GFP/BH3-Ct fusions, HeLa cells were incubated at 37ºC with Mitotracker red dye 500 nM (Thermo scientific ref. M7512) and DAPI (4',6-diamidino-2-phenylindole, Thermo scientific ref. D1306) for 30 min. Microscopic images of living cells were taken 24 hours after transfection using confocal microscopy at 25ºC (Leica TCS SP2 AOBS) with a 63x oil 1.4 objective, using zoom 3 and 1024x1024 pixels resolution. Immersion oil Leica Type F (ref. 11513859) with refractive index at 22ºC n=1.5180. Blue diode laser for 405nm, laser He/Ne 594nm. Argon laser for 488nm excitation.

For the ER localization and cyt *c* release assay, after cell attachment, cell spreading, and transfection with the GFP/BH3-Ct constructs, HeLa cells were fixed with 4% paraformaldehyde for 20 min. After three washes with PBS, cells were permeabilized with 0.1% Triton X-100 for 10 min and blocked in 2% gelatin PBS for 30 min. Cells were then labeled with antibodies against cyt-*c* (1:200; SC13561; Santa Cruz) and Grp78 protein (1:400; ab21685; Abcam) in PBS plus 2% gelatin followed by incubation with an anti-mouse IgG-Alexa 555 (1:400) secondary antibody also in PBS plus 2% gelatin (Invitrogen). Coverslips were mounted on glass slides with 5 µL of Mowiol/Dapi (nuclear marker, 5 µg/ml) (Sigma). Images were obtained using confocal microscopy (see above) with a 63x objective (green channel, λ_{exc} 488 nm, λ_{emi} 515 nm; red channel, λ_{exc} 561 nm, λ_{emi} 598 nm). Fluorescence images were analyzed with ImageJ 1.46i "JACoP plugin" with contrast and gamma adjustments according to the provider's instructions. All background fluorescence was eliminated to avoid false-positives. Co-localization was defined as completely overlapping or partially overlapping signals. All experiments were repeated three times. At least 30 images of each sample were analyzed.

Immunoblotting the GFP/BH3-Ct fusion proteins in HeLa cells – After 24 h of GFP/BH3-Ct transfection, whole cell extracts were obtained by lysing cells in buffer containing 25 mM Tris-HCl pH 7.4, 1 mM EDTA, 1 mM EGTA, 1% SDS, and protease and phosphatase inhibitors. The total protein was quantified using the BCA protein assay kit (Thermo Scientific), and 50 µg of the whole protein extract was dissolved in protein loading buffer (Tris-HCl pH 6.8, 10% w/v SDS, 250 mM DTT, 0.03% w/v bromophenol blue, and 50% v/v glycerol) and boiled 5 min at 95ºC. Proteins were resolved by

SDS-PAGE (acrylamide 12%) and transferred to nitrocellulose membranes, and the membranes were blocked with 5% non-fat milk, washed three times with TBS-Tween 20 (0.1%), and incubated overnight at 4°C with specific primary antibodies against GFP (1:1000, ab13970, Abcam) and α-tubulin (1:1000, #T8203, Sigma-Aldrich). The membranes were then washed with TBS-Tween 20 (0.1%) and probed with the appropriate secondary antibody: α-mouse (1:3000, A4937, Sigma) or α-rabbit (1:3000,A0545, Sigma) conjugated to horseradish peroxidase for enhanced chemiluminescence detection (Amersham Pharmacia Biotech).

Caspase-like activity assay – All cell extracts were prepared from 2×10^5 cells that were seeded in 6-well plates. After 24 h, cells were treated and/or transfected as indicated above; 24 h after this, the cells were scraped, washed with PBS, and collected by centrifugation at 500×g. The pellets were resuspended in caspase assay buffer (PBS with 10% glycerol, 0.1 mM EDTA, and 2 mM DTT) supplemented with protease inhibitor cocktail (Sigma) and kept on ice for 5 min. The pellets were frozen and thawed three times in liquid nitrogen, the cell lysates were centrifuged at 14,000 rpm for 5 min, and the supernatants were collected. Quantification of the total protein concentration was performed using the BCA protein assay kit. Total protein (50 μg) was mixed with 200 μL of caspase assay buffer (PBS with 10% glycerol, 0.1 mM EDTA, and 2 mM DTT) containing 20 μM of the Ac-DEVD-AFC (Enzo Life Sciences) caspase-3-specific substrate. Caspase activity was monitored continuously following the release of fluorescent AFC at 37°C using a Wallac 1420 Workstation (λexc, 400 nm; λem, 508 nm). Caspase-3 activity was expressed as the increase of relative fluorescence units per min (A.U.)

Statistical analyses – Bars represent the mean ± s.d. of at least three independent experiments.

Acknowledgments: We thank Prof. Donald M. Engelman of Yale University for providing the ToxR vector and the *E. coli* MM39 (DE3) cells.

Conflict of interest: The authors declare that they have no conflicts of interest with the contents of this article.

Author contributions: IM conceived and coordinated the study, and wrote the paper. VAF, MJGM and MBP designed, performed and analyzed the experiments shown in Figures 1 and 2. JM and LM designed and carried out the molecular dynamics simulations (Fig. 3). VAF and MO designed, performed and analyzed the experiments shown in Figures 4 and 5. All authors reviewed the results, edited the manuscript and approved the final version of the manuscript.

REFERENCES

1. Doerflinger, M., Glab, J. A., and Puthalakath, H. (2015) BH3-only proteins: a 20-year stock-take. FEBS J 282, 1006-1016
2. Kim, H., Rafiuddin-Shah, M., Tu, H. C., Jeffers, J. R., Zambetti, G. P., Hsieh, J. J., and Cheng, E. H. (2006) Hierarchical regulation of mitochondrion-dependent apoptosis by BCL-2 subfamilies. Nature cell biology 8, 1348-1358
3. Chen, H. C., Kanai, M., Inoue-Yamauchi, A., Tu, H. C., Huang, Y., Ren, D., Kim, H., Takeda, S., Reyna, D. E., Chan, P. M., Ganesan, Y. T., Liao, C. P., Gavathiotis, E., Hsieh, J. J., and Cheng, E. H. (2015) An interconnected hierarchical model of cell death regulation by the BCL-2 family. Nature cell biology 17, 1270-1281
4. Letai, A., Bassik, M. C., Walensky, L. D., Sorcinelli, M. D., Weiler, S., and Korsmeyer, S. J. (2002) Distinct BH3 domains either sensitize or activate mitochondrial apoptosis, serving as prototype cancer therapeutics. Cancer cell 2, 183-192
5. Uren, R. T., Dewson, G., Chen, L., Coyne, S. C., Huang, D. C., Adams, J. M., and Kluck, R. M. (2007) Mitochondrial permeabilization relies on BH3 ligands engaging multiple prosurvival Bcl-2 relatives, not Bak. J Cell Biol 177, 277-287
6. Gomez-Fernandez, J. C. (2014) Functions of the C-terminal domains of apoptosis-related proteins of the Bcl-2 family. Chemistry and physics of lipids 183C, 77-90
7. Andreu-Fernandez, V., Genoves, A., Lee, T. H., Stellato, M., Lucantoni, F., Orzaez, M., Mingarro, I., Aguilar, M. I., and Perez-Paya, E. (2014) Peptides derived from the transmembrane domain of bcl-2 proteins as potential mitochondrial priming tools. ACS chemical biology 9, 1799-1811
8. Aranovich, A., Liu, Q., Collins, T., Geng, F., Dixit, S., Leber, B., and Andrews, D. W. (2012) Differences in the mechanisms of proapoptotic BH3 proteins binding to Bcl-XL and Bcl-2 quantified in live MCF-7 cells. Mol Cell 45, 754-763
9. Wilfling, F., Weber, A., Potthoff, S., Vogtle, F. N., Meisinger, C., Paschen, S. A., and Hacker, G. (2012) BH3-only proteins are tail-anchored in the outer mitochondrial membrane and can initiate the activation of Bax. Cell death and differentiation 19, 1328-1336
10. Czabotar, P. E., Lessene, G., Strasser, A., and Adams, J. M. (2014) Control of apoptosis by the BCL-2 protein family: implications for physiology and therapy. Nat Rev Mol Cell Biol 15, 49-63
11. Yao, Y., Fujimoto, L. M., Hirshman, N., Bobkov, A. A., Antignani, A., Youle, R. J., and Marassi, F. M. (2015) Conformation of BCL-XL upon Membrane Integration. J Mol Biol 427, 2262-2270
12. Hessa, T., Kim, H., Bihlmaier, K., Lundin, C., Boekel, J., Andersson, H., Nilsson, I., White, S. H., and von Heijne, G. (2005) Recognition of transmembrane helices by the endoplasmic reticulum translocon. Nature 433, 377-381
13. Hessa, T., Meindl-Beinker, N. M., Bernsel, A., Kim, H., Sato, Y., Lerch-Bader, M., Nilsson, I., White, S. H., and von Heijne, G. (2007) Molecular code for transmembrane-helix recognition by the Sec61 translocon. Nature 450, 1026-1030
14. Bano-Polo, M., Martinez-Gil, L., Wallner, B., Nieva, J. L., Elofsson, A., and Mingarro, I. (2013) Charge pair interactions in transmembrane helices and turn propensity of the connecting sequence promote helical hairpin insertion. J Mol Biol 425, 830-840
15. Bano-Polo, M., Baeza-Delgado, C., Orzaez, M., Marti-Renom, M. A., Abad, C., and Mingarro, I. (2012) Polar/Ionizable residues in transmembrane segments: effects on helix-helix packing. PLoS One 7, e44263
16. Berger, B. W., Kulp, D. W., Span, L. M., DeGrado, J. L., Billings, P. C., Senes, A., Bennett, J. S., and DeGrado, W. F. (2010) Consensus motif for integrin transmembrane helix association. Proc Natl Acad Sci U S A 107, 703-708
17. Russ, W. P., and Engelman, D. M. (1999) TOXCAT: a mesure of transmembrane helix association in a biological membrane. Proc Natl Acad Sci USA 96, 863-868

18. Marrink, S. J., Risselada, H. J., Yefimov, S., Tieleman, D. P., and de Vries, A. H. (2007) The MARTINI force field: Coarse grained model for biomolecular simulations. J. Phys. Chem. B 111, 7812-7824
19. Monticelli, L., Kandasamy, S. K., Periole, X., Larson, R. G., Tieleman, D. P., and Marrink, S. J. (2008) The MARTINI coarse-grained force field: Extension to proteins. Journal of Chemical Theory and Computation 4, 819-834
20. Yesylevskyy, S. O., Schafer, L. V., Sengupta, D., and Marrink, S. J. (2010) Polarizable Water Model for the Coarse-Grained MARTINI Force Field. PLoS Computational Biology 6
21. Hess, B., Kutzner, C., van der Spoel, D., and Lindahl, E. (2008) GROMACS 4: Algorithms for highly efficient, load-balanced, and scalable molecular simulation. Journal of Chemical Theory and Computation 4, 435-447
22. Abraham, M. J., Murtola, T., Schulz, R., Páll, S., Smith, J. C., Hess, B., and Lindahl, E. (2015) GROMACS: High performance molecular simulations through multi-level parallelism from laptops to supercomputers. SoftwareX 1–2, 19-25
23. Pall, S., and Hess, B. (2013) A flexible algorithm for calculating pair interactions on SIMD architectures. Computer Physics Communications 184, 2641-2650
24. Marrink, S. J., and Tieleman, D. P. (2013) Perspective on the Martini model. Chemical Society Reviews 42, 6801-6822
25. Darden, T., York, D., and Pedersen, L. (1993) Particle mesh Ewald: an N-log(N) method for Ewald sums in large systems. Journal of Chemical Physics 98, 10089-10092
26. Essmann, U., Perera, L., Berkowitz, M. L., Darden, T., Lee, H., and Pedersen, L. G. (1995) A smooth particle mesh Ewald potential. Journal of Chemical Physics 103, 8577-8592
27. Bussi, G., Donadio, D., and Parrinello, M. (2007) Canonical sampling through velocity rescaling. Journal of Chemical Physics 126, 014101
28. Berendsen, H. J. C., Postma, J. P. M., van Gunsteren, W. F., di Nola, A., and Haak, J. R. (1984) Molecular dynamics with coupling to an external bath. Journal of Chemical Physics 81, 3684-3690
29. Shamas-Din, A., Kale, J., Leber, B., and Andrews, D. W. (2013) Mechanisms of action of Bcl-2 family proteins. Cold Spring Harbor perspectives in biology 5, a008714
30. Martinez-Gil, L., Perez-Gil, J., and Mingarro, I. (2008) The surfactant peptide KL4 sequence is inserted with a transmembrane orientation into the endoplasmic reticulum membrane. Biophys J 95, L36-38
31. Martinez-Gil, L., Sauri, A., Vilar, M., Pallas, V., and Mingarro, I. (2007) Membrane insertion and topology of the p7B movement protein of Melon Necrotic Spot Virus (MNSV). Virology 367, 348-357
32. Tamborero, S., Vilar, M., Martinez-Gil, L., Johnson, A. E., and Mingarro, I. (2011) Membrane Insertion and Topology of the Translocating Chain-Associating Membrane Protein (TRAM). J Mol Biol 406, 571-582
33. Garcia-Saez, A. J., Mingarro, I., Perez-Paya, E., and Salgado, J. (2004) Membrane-insertion fragments of Bcl-xL, Bax, and Bid. Biochemistry 43, 10930-10943
34. Shamas-Din, A., Brahmbhatt, H., Leber, B., and Andrews, D. W. (2011) BH3-only proteins: Orchestrators of apoptosis. Biochim Biophys Acta 1813, 508-520
35. Lithgow, T., van Driel, R., Bertram, J. F., and Strasser, A. (1994) The protein product of the oncogene bcl-2 is a component of the nuclear envelope, the endoplasmic reticulum, and the outer mitochondrial membrane. Cell Growth Differ 5, 411-417
36. Germain, M., Mathai, J. P., and Shore, G. C. (2002) BH-3-only BIK functions at the endoplasmic reticulum to stimulate cytochrome c release from mitochondria. J Biol Chem 277, 18053-18060
37. Pang, X., Zhang, J., Lopez, H., Wang, Y., Li, W., O'Neill, K. L., Evans, J. J., George, N. M., Long, J., Chen, Y., and Luo, X. (2014) The carboxyl-terminal tail of Noxa protein regulates the stability of Noxa and Mcl-1. J Biol Chem 289, 17802-17811
38. Zheng, J. Y., Tsai, Y. C., Kadimcherla, P., Zhang, R., Shi, J., Oyler, G. A., and Boustany, N. N. (2008) The C-terminal transmembrane domain of Bcl-xL mediates changes in mitochondrial morphology. Biophys J 94, 286-297

39. Tatulian, S. A., Garg, P., Nemec, K. N., Chen, B., and Khaled, A. R. (2012) Molecular basis for membrane pore formation by Bax protein carboxyl terminus. Biochemistry 51, 9406-9419
40. Kvansakul, M., and Hinds, M. G. (2014) The Structural Biology of BH3-Only Proteins. Methods in enzymology 544, 49-74
41. Moldoveanu, T., Follis, A. V., Kriwacki, R. W., and Green, D. R. (2014) Many players in BCL-2 family affairs. Trends in biochemical sciences 39, 101-111
42. Lindsay, J., Esposti, M. D., and Gilmore, A. P. (2011) Bcl-2 proteins and mitochondria--specificity in membrane targeting for death. Biochim Biophys Acta 1813, 532-539
43. Kaufmann, T., Schlipf, S., Sanz, J., Neubert, K., Stein, R., and Borner, C. (2003) Characterization of the signal that directs Bcl-x(L), but not Bcl-2, to the mitochondrial outer membrane. J Cell Biol 160, 53-64
44. Woolfson, D. N., and Williams, D. H. (1990) The influence of proline residues on a-helical structure. FEBS Lett 277, 185-188
45. Orzaez, M., Salgado, J., Gimenez-Giner, A., Perez-Paya, E., and Mingarro, I. (2004) Influence of proline residues in transmembrane helix packing. J Mol Biol 335, 631-640
46. Baeza-Delgado, C., von Heijne, G., Marti-Renom, M. A., and Mingarro, I. (2016) Biological insertion of computationally designed short transmembrane segments. Scientific Reports 6, 23397
47. Jaud, S., Fernandez-Vidal, M., Nilsson, I., Meindl-Beinker, N. M., Hubner, N. C., Tobias, D. J., von Heijne, G., and White, S. H. (2009) Insertion of short transmembrane helices by the Sec61 translocon. Proc Natl Acad Sci U S A 106, 11588-11593
48. Zhu, Y., Swanson, B. J., Wang, M., Hildeman, D. A., Schaefer, B. C., Liu, X., Suzuki, H., Mihara, K., Kappler, J., and Marrack, P. (2004) Constitutive association of the proapoptotic protein Bim with Bcl-2-related proteins on mitochondria in T cells. Proc Natl Acad Sci U S A 101, 7681-7686
49. Ren, D., Tu, H. C., Kim, H., Wang, G. X., Bean, G. R., Takeuchi, O., Jeffers, J. R., Zambetti, G. P., Hsieh, J. J., and Cheng, E. H. (2010) BID, BIM, and PUMA are essential for activation of the BAX- and BAK-dependent cell death program. Science 330, 1390-1393
50. Hinds, M. G., Smits, C., Fredericks-Short, R., Risk, J. M., Bailey, M., Huang, D. C., and Day, C. L. (2007) Bim, Bad and Bmf: intrinsically unstructured BH3-only proteins that undergo a localized conformational change upon binding to prosurvival Bcl-2 targets. Cell death and differentiation 14, 128-136
51. Hill, R. B., MacKenzie, K. R., and Harwig, M. C. (2015) The Tail-End Is Only the Beginning: NMR Study Reveals a Membrane-Bound State of BCL-XL. J Mol Biol 427, 2257-2261
52. Grespi, F., Soratroi, C., Krumschnabel, G., Sohm, B., Ploner, C., Geley, S., Hengst, L., Hacker, G., and Villunger, A. (2010) BH3-only protein Bmf mediates apoptosis upon inhibition of CAP-dependent protein synthesis. Cell death and differentiation 17, 1672-1683
53. Grimm, S. (2012) The ER-mitochondria interface: the social network of cell death. Biochim Biophys Acta 1823, 327-334

FOOTNOTES

This work was supported by grants #PROMETEOII/2014/061 from the Generalitat Valenciana and #BFU2016-79487 from the Spanish Ministry of Economics and Competitiveness.

The abbreviations used are: Bcl-2, B-cell lymphoma-2; BH3, Bcl-2 homology-3; C-terminus, carboxyl-terminus; GFP, green fluorescence protein; MBP, maltose binding protein; MOM, mitochondrial outer membrane; MOMP, mitochondrial outer membrane permeabilization.

FIGURE LEGENDS

Figure 1. Insertion of BH3-only C-termini into microsomal membranes. (A) Schematic of the engineered leader peptidase (Lep) model protein. G1 and G2 denote artificial glycosylation acceptor sites. (B) and (C) *In vitro* protein translation in the presence (+) or absence (−) of rough

microsomes (RM) and proteinase K (PK). Non-glycosylated protein bands are indicated by a white dot; single and double glycosylated protein bands are indicated by one or two black dots, respectively. A black triangle indicates protected glycosylated H2/P2 or BH3-Ct/P2 fragments.

Figure 2. The maltose complementation assay for transmembrane insertion and orientation. (A) Schematic of the engineered cytoplasmic ToxR and periplasmic maltose binding protein (MBP) domains that were fused to BH3-only protein C-terminal regions at the N- and C-termini, respectively. (B) *malE*-deficient *E. coli* MM39 cells were transformed with the indicated expression constructs and cultured on M9 agar containing 0.4% maltose. (C) Expression of all constructs was verified by growing the MM39 *malE*-deficient *E. coli* cells in complete LB media with the appropriate antibiotic selection (ampicillin), and by Western blot analysis (anti-MBP) of the constructs containing apoptotic C-terminal regions (bottom panel). Positive controls, ToxR(Bax α9)MBP and ToxR(Bcl-2 α9)MBP; negative control, ToxR(ΔTM)MBP.

Figure 3. (A) Snapshots from molecular dynamics (MD) simulations of Bik in DOPC lipids. The peptide can show interfacial (top) or transmembrane (bottom) orientation. (B) Peptide orientation distributions. For each peptide and for each simulation, we calculated the component of the principal axis of inertia in the direction of the membrane normal (defined as the Z direction) at the end of the self-assembly simulation. If the peptide has a transmembrane orientation (yellow), its principal axis of inertia has a Z component close to 1; if the peptide lies parallel to the membrane surface (gray), the Z component is close to 0. Each plot shows the distribution of the Z component of the principal axis of inertia in all self-assembly simulations (100 for each peptide).

Figure 4. Intracellular localization of GFP/BH3-Ct fusions as analyzed by confocal microscopy. The C-terminal sequences (Table 1) of BH3-only proteins were fused to the C-terminus of GFP and the constructs were transiently expressed in HeLa cells. Intracellular localization of the GFP/BH3-Ct fusion proteins (green channel) was analyzed by microscopy. Cells were incubated with Mitotracker (A) and anti-Grp78 (B) as mitochondrial and ER markers, respectively (red channel). Co-localizations are shown in yellow. The images in boxes are shown at higher magnification in the last column (inset). The bars represent either 20 μm or 2 μm (inset).

Figure 5. GFP/BH3-Ct fusions do not promote apoptosis activation in healthy cells. Caspase-3/7-like activity was measured in HeLa cells. Bars represent the means of three experiments ± s.d. ABT-263 (10 μM) was used as a positive control for apoptosis induction. The Western blots (bottom) used antibodies to GFP and α-tubulin as loading controls.

Table 1: Thermodynamic cost of BH3-only C-terminal domains integration. Analyzed protein sequences using ΔG Prediction Server v1.0 (http://dgpred.cbr.su.se/). Subsequences with lowest ΔG marked in orange as predicted by the algorithm. ΔG values are expressed in kcal/mol, both for the predicted (third column) and the experimental data (forth column). Negative and positive ΔG values are shown in green and red, respectively and denote spontaneous insertion or non-insertion, respectively. The probability of insertion (P_i) has been calculated from the experimental data as previously described (12,32). Predictions of peptide insertion based on MD simulations with the MARTINI model (fifth and sixth columns). Probabilities (%) are calculated simply from counting the instances of TM *vs*. interfacial peptide orientation observed in the simulations. M2.2 indicates MARTINI v2.2, while M2.2P indicates MARTINI v2.2 with polarizable water and long-range electrostatics (see Methods). Puma simulations for fully helical peptides were compared with the simulations of peptides in which the helix was restricted (probabilities in parenthesis) to the residues found between Pro167 and Pro180 (shown in bold) from human sequence. Probabilities above and below 50% are shown in green and red, respectively, for consistency.

Protein	Sequence	pred ΔG_{app}	exp ΔG_{app}	P_i (%)	M2.2 sim	M2.2P sim
Lep-H2	WLETGASVFPVLAIVIIVRSFIY	−0.0	−1.1	85.9	60	68
Bik-Ct	LLALLLLLALLLPLLSGGLHLLL	−2.9	−0.8	77.8	68	67
Bim-Ct	EDHPRMMILRLLRYIVRLVWRMH	+2.8	+0.7	23.2	45	42
Noxa-Ct	FGDKLNFRQKLLNLISKLFCSGT	+5.5	+2.6	1.4	37	43
Bmf-Ct	QNRVWWQILLFLHNLALNGEENI	+2.1	−0.3	60.4	65	57
Puma-Ct	RPSPWRVLYNLIMGLLPLPRGHR	+2.6	+0.4	35.4	67(42)	70(45)

Figure 1

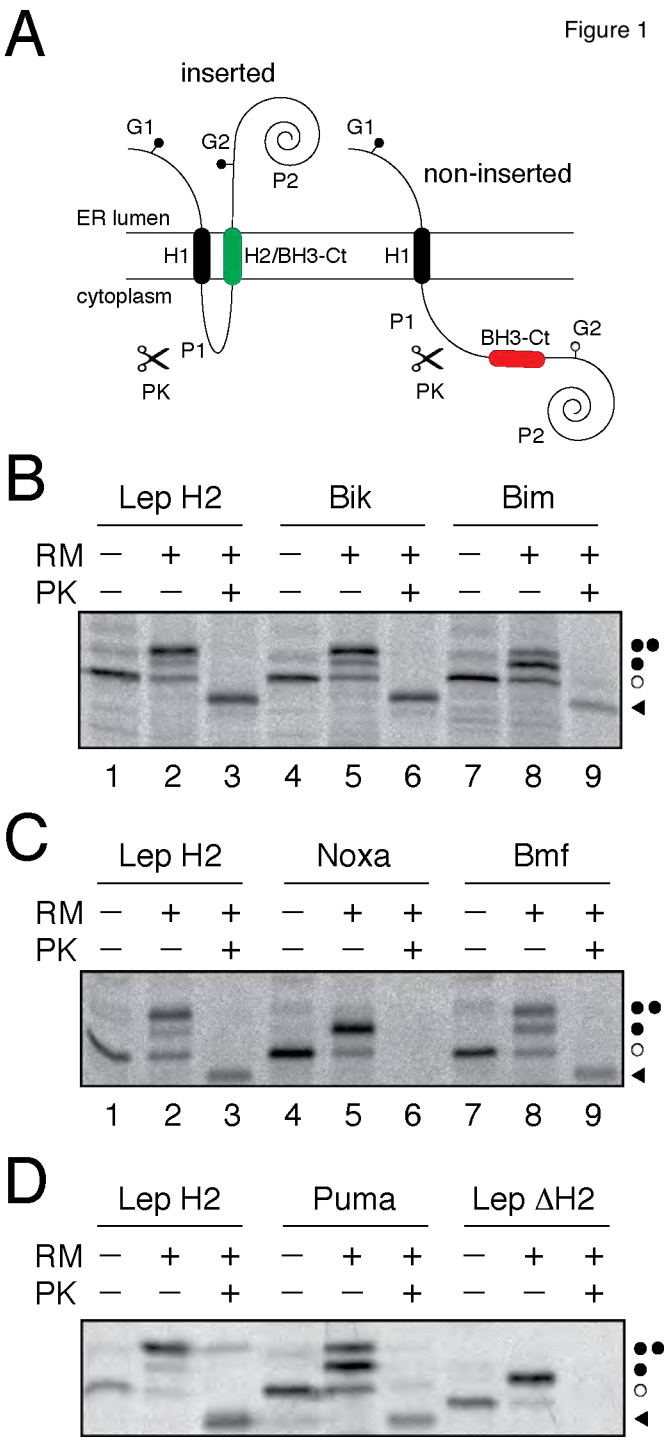

Figure 2

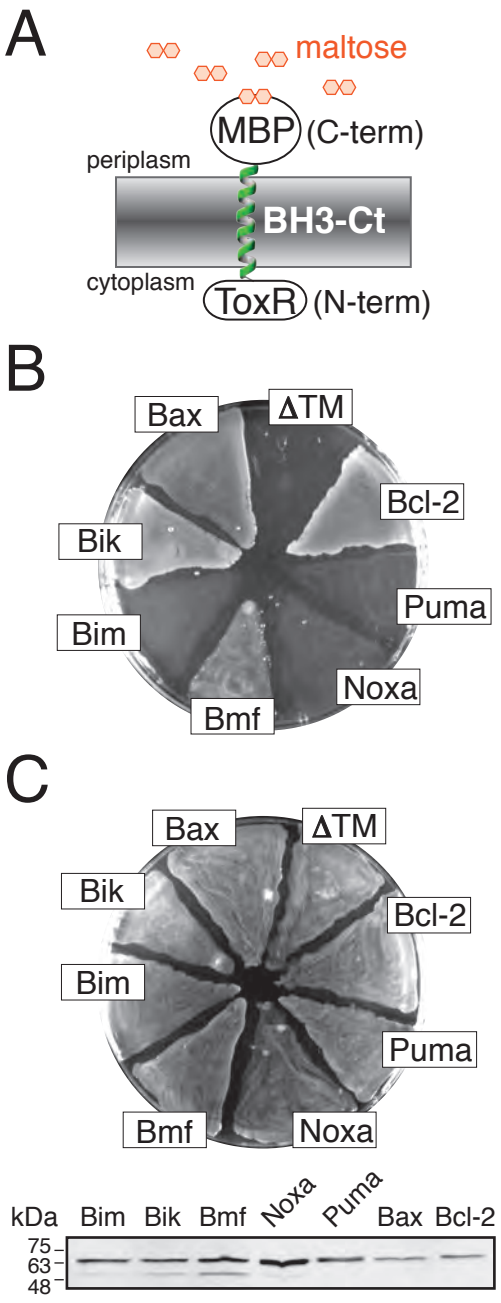

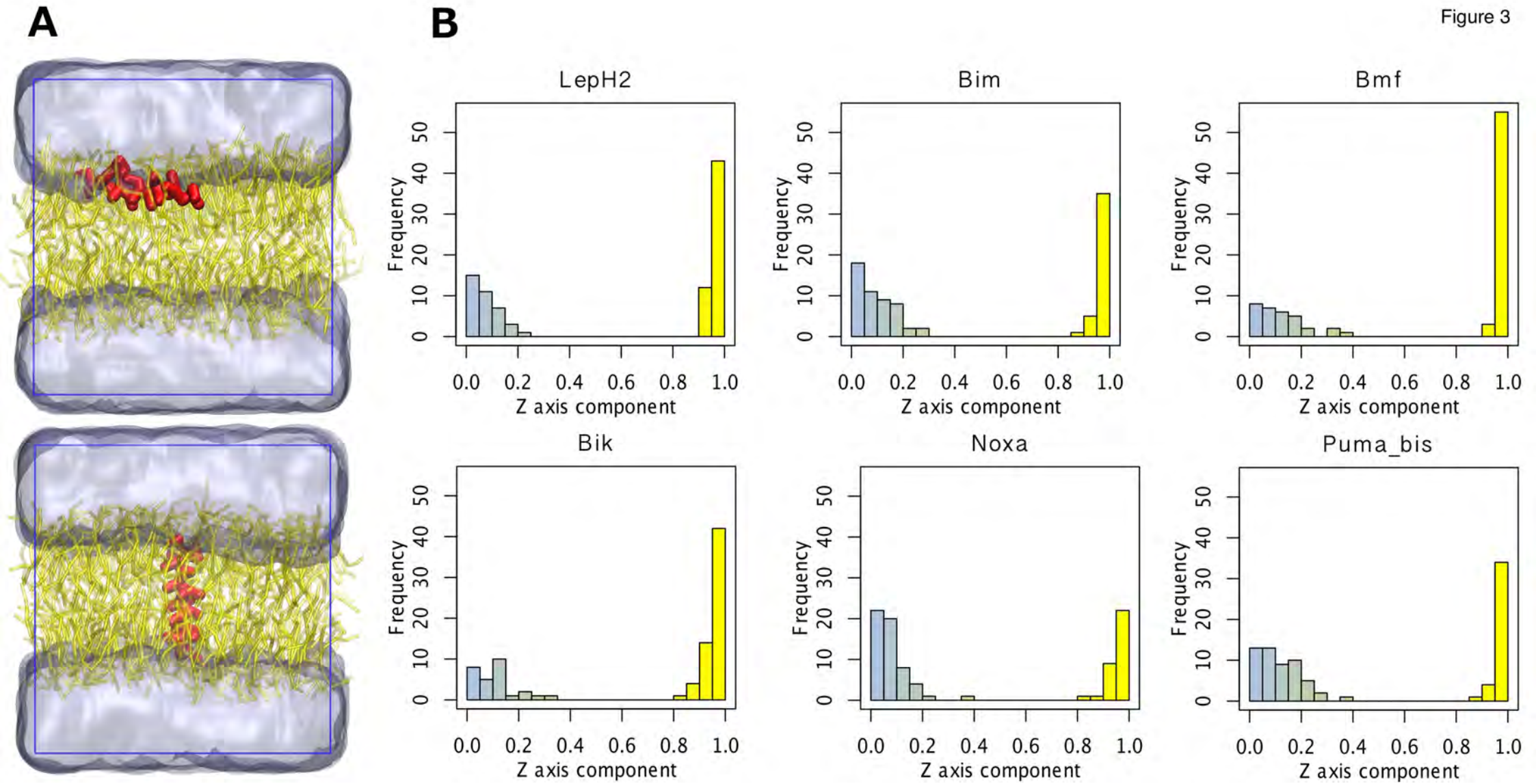

Figure 3

Figure 4A

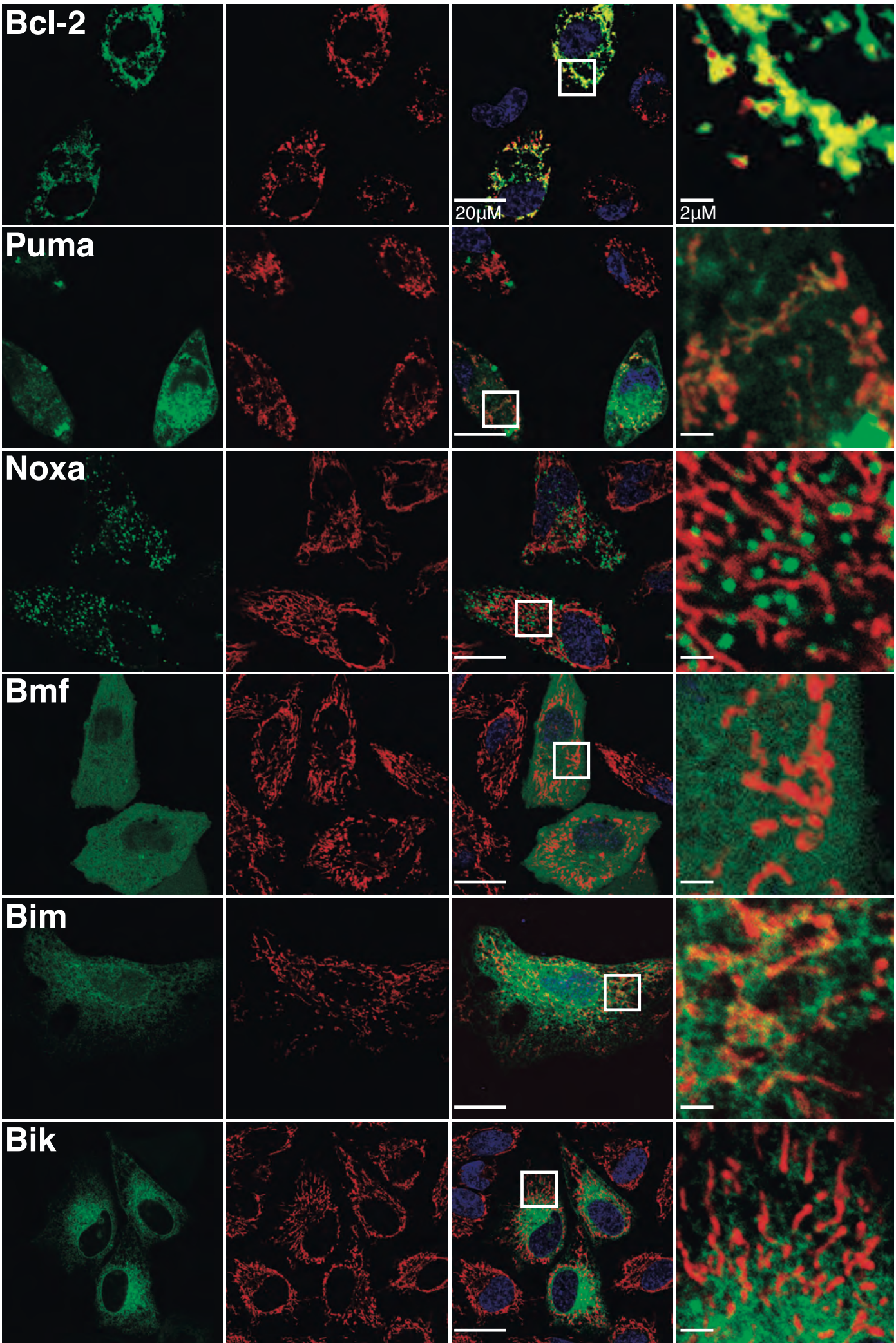

Figure 4B

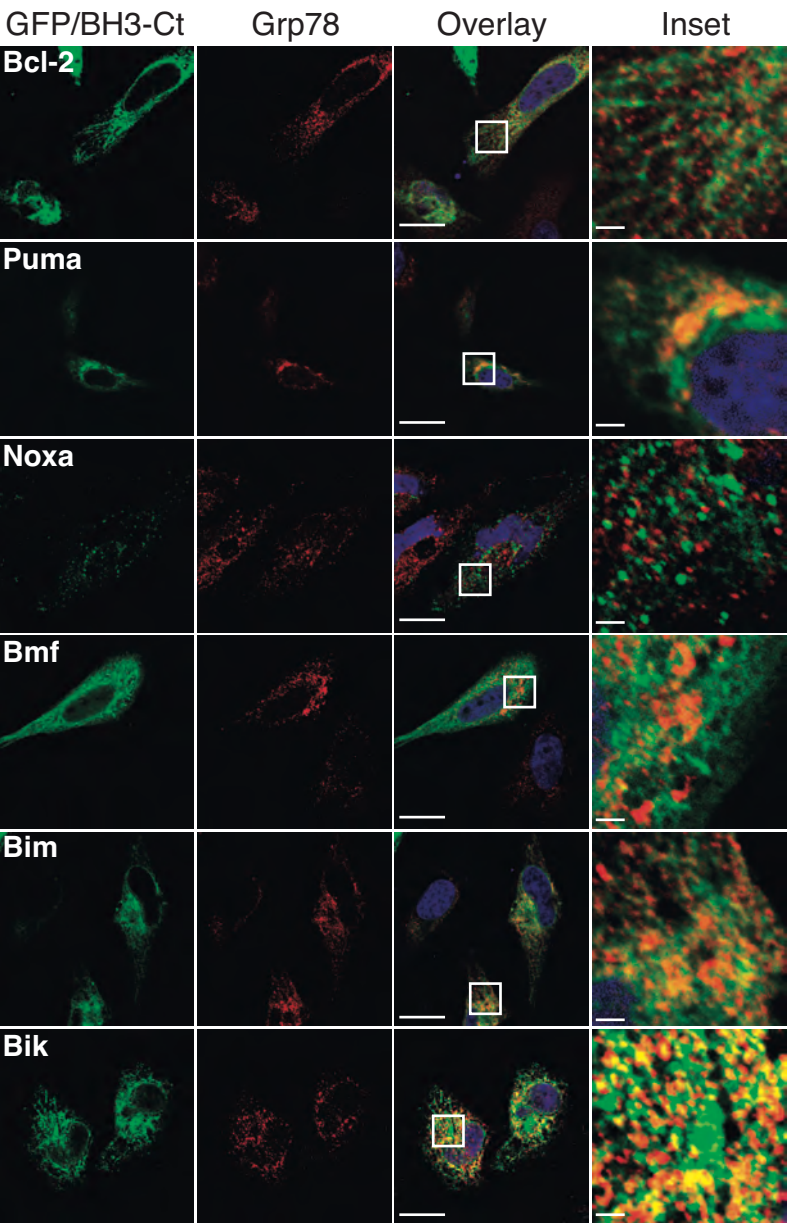

Figure 5

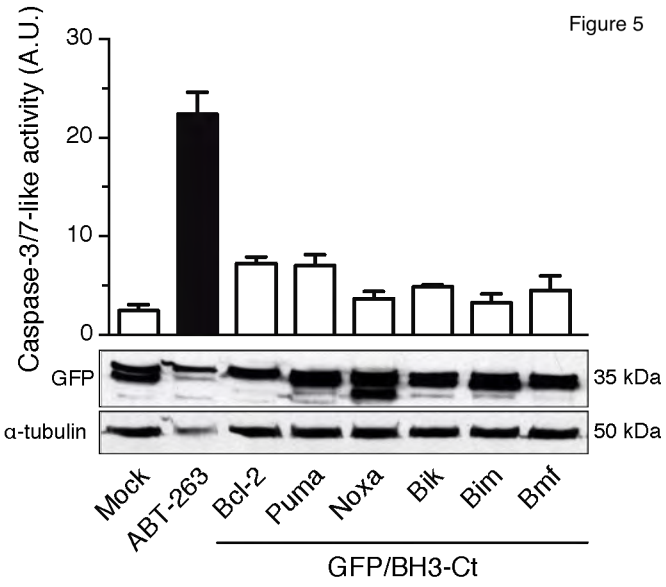

The C-terminal domains of apoptotic BH3-only proteins mediate their insertion into distinct biological membranes

Vicente Andreu-Fernandez, Maria J. García-Murria, Manuel Bañó-Polo, Juliette Martin, Luca Monticelli, Mar Orzáez and Ismael Mingarro

J. Biol. Chem. published online October 7, 2016